ARTICLE

Synergistic Speed Enhancement of an Electric-Photochemical Hybrid Micromotor by Tilt Rectification

Zuyao Xiao, Shifang Duan, Pengzhao Xu, Jingqin Cui, Hepeng Zhang, and Wei Wang*

Cite This: https://dx.doi.org/10.1021/acsnano.0c03022

Read Online

ACCESS | Metrics & More | Article Recommendations | Supporting Information

ABSTRACT: A hybrid micromotor is an active colloid powered by more than one power source, often exhibiting expanded functionality and controllability than those of a singular energy source. However, these power sources are often applied orthogonally, leading to stacked propulsion that is just a sum of two independent mechanisms. Here, we report that TiO_2–Pt Janus micromotors, when subject to both UV light and AC electric fields, move up to 90% faster than simply adding up the speed powered by either source. This unexpected synergy between light and electric fields, we propose, arises from the fact that an electrokinetically powered TiO_2–Pt micromotor moves near a substrate with a tilted Janus interface that, upon the application of an electric field, becomes rectified to be vertical to the substrate. Control experiments with magnetic fields and three types of micromotors unambiguously and quantitatively show that the tilting angle of a micromotor correlates positively with its instantaneous speed, reaching maximum at a vertical Janus interface. Such "tilting-induced retardation" could affect a wide variety of chemically powered micromotors, and our findings are therefore helpful in understanding the dynamics of micromachines in confinement.

KEYWORDS: micromotor, ICEP, photoactive, Janus interface, acceleration
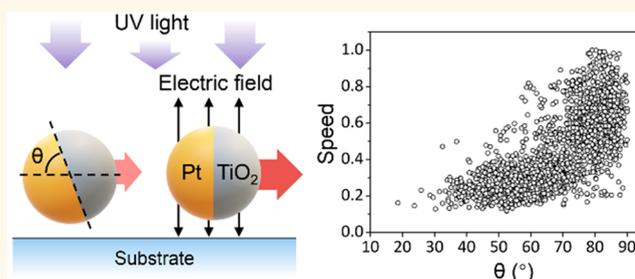
Micromotors are an emerging class of colloids that move autonomously by harvesting energy stored in the environment in the form of chemicals, electromagnetic waves, heat, or sound.[1−5] Also known as micromachines,[2] microbots,[6] synthetic microswimmers,[7] or active colloids[8] in different contexts, micromotors hold great promise both in applied scenarios such as biomedical or environmental applications[9,10] and in fundamental sciences as a model system for the study of active matter.[11] As research in both the applied and fundamental fronts has progressed over the last two decades or so, micromotors are increasingly exposed to more complex environments,[12,13] calling for innovative designs that unlock more functionalities and better control capabilities.

The recent development of the so-called "hybrid" micromotors comes into focus.[14] Considering the various sources of energy a micromotor can exploit, a hybrid micromotor, one activated by more than one power source, can accelerate/decelerate, move forward/backward, or switch modes of motion, upon switching between two or more different driving forces (see a recent review[14] and refs therein). Examples include TiO_2–Pt micromotors that move both under light and in H_2O_2 via two mechanisms and in opposite directions[15] and AuRu bimetallic rods that can be powered by either ultrasound

or H_2O_2.[16] The design of these hybrid micromotors confers some unique advantages, such as a higher degree of motion control, stronger propulsion, and the ability of switching to a second type of fuel when the first one is depleted. A typical feature of existing hybrid micromotors, however, is that the two power sources are applied orthogonally, meaning that they can be turned on and off independently without significantly interfering with each other. Therefore, the dynamics of a hybrid micromotor is often a result of the vector sum of the two driving forces, a "1 + 1 = 2" scenario.

We here report how this simple 1 + 1 = 2 scenario breaks down, where *simultaneously* applying light and an alternating current (AC) electric field drives a photocatalytic titania-platinum (TiO_2–Pt) micromotor at a speed that is, in the most extreme case, ~90% faster than simply adding up its speed
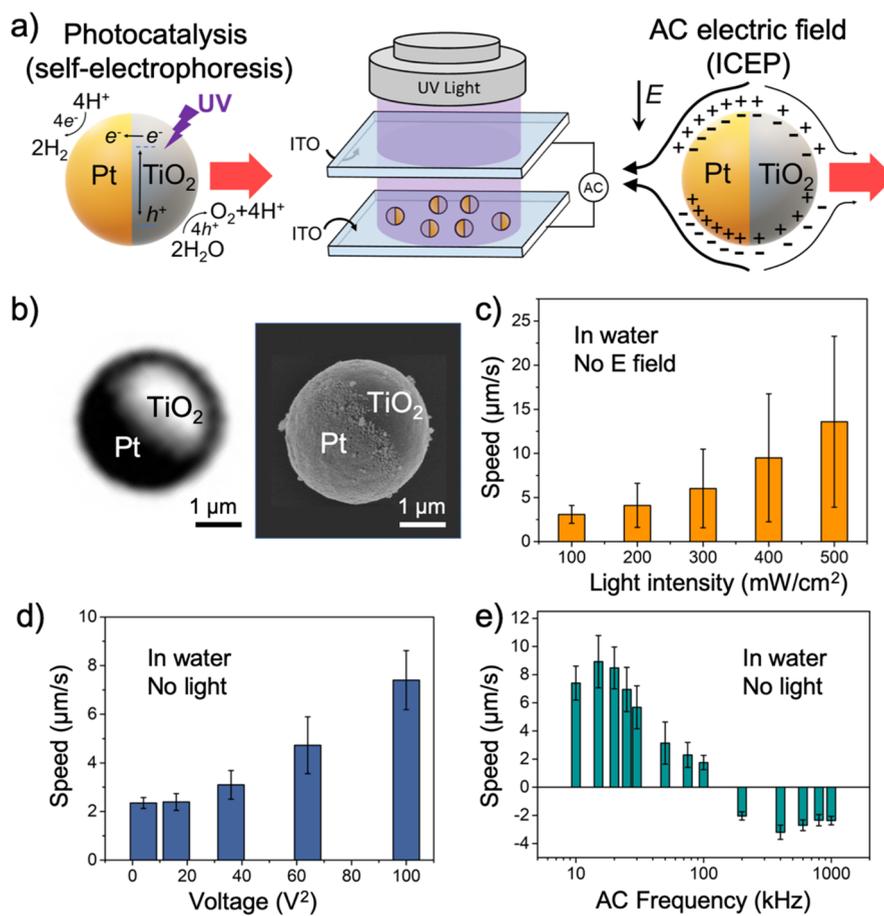
Figure 1. Propulsion of a TiO₂−Pt micromotor powered by individual sources. (a) Operating principles of a TiO₂−Pt hybrid micromotor. (left) Photocatalytic self-electrophoresis under UV light illumination. (right) Induced charge electrophoresis, or ICEP, under an AC electric field. (center) Experiment setup for applying both the UV light and an AC electric field to a population of TiO₂−Pt Janus microspheres. (b) Optical micrograph (left) and scanning electron micrograph (right) of a TiO₂−Pt Janus microsphere. (c) Speeds of a TiO₂−Pt micromotor increase as the light intensity increases. (d, e) Speeds of a TiO₂−Pt micromotor increase as the driving voltages of an AC electric field increase (d) but reverse signs as the driving frequencies increase beyond ∼100 kHz (at 10 V).

under either propulsion; that is, 1 + 1 > 2. We propose that such a synergy arises from the fact that a phoretically powered micromotor moves near a substrate at a tilted angle (a zenith angle less than 90°, see below), which turns out to significantly reduce the micromotor speed, an effect we term "tilting-induced retardation". When an electric field is applied perpendicular to the substrate, the tilting is rectified, returning a micromotor to its unretarded speed. Our finding also holds valid for experiments where magnetic fields rather than electric fields were used to modulate the tilting angle, as well as experiments with Pt-coated Janus micromotors that were not light-responsive, suggesting that tilting-induced retardation could be a universal feature for micromotors powered by chemical gradients. This study therefore has far-reaching implications in not only improving the performance and efficiency of chemical micromotors but also understanding the often-complicated interactions between active colloids with a confining environment.[13,17]

RESULTS/DISCUSSION

We begin with a brief introduction to the experimental design and operating principles of the hybrid micromotors studied here (Figure 1). As mentioned earlier, TiO₂−Pt Janus microspheres are exposed to both light and AC electric fields

to act as a hybrid micromotor. More specifically, TiO₂−Pt Janus microspheres are known to move under UV light (Figure 1a, left),[18−22] where the photogenerated electron−hole pairs oxidize and reduce water on the Pt and TiO₂ hemispheres, respectively, generating an excess of protons near the TiO₂ cap and a shortage of protons near the Pt cap. On the one hand, the proton gradient arising from this water splitting then creates a self-generated electric field that drives the particle, a mechanism known as self-electrophoresis. On the other hand, a TiO₂−Pt microsphere, being a metal-dielectric Janus particle, also moves under an AC electric field (Figure 1a, right) by a completely different mechanism.[23−29] In this scenario, a polarizable material generates an electro-osmotic flow on its surface because of charges induced by the externally applied electric fields. Since the two hemispheres of a TiO₂−Pt microsphere polarize very differently in the electric field, the induced charge electro-osmosis (ICEO) is of different magnitudes on the two surfaces, giving rise to an asymmetric flow that moves the particle forward, a propulsion mechanism called induced charge electrophoresis (ICEP). Both mechanisms, self-electrophoresis under UV light and ICEP under AC electric fields, are well-documented and propel the particle toward the same direction, TiO₂ forward.

This hybrid motor design is experimentally implemented as follows. TiO₂−Pt Janus microparticles were prepared by first
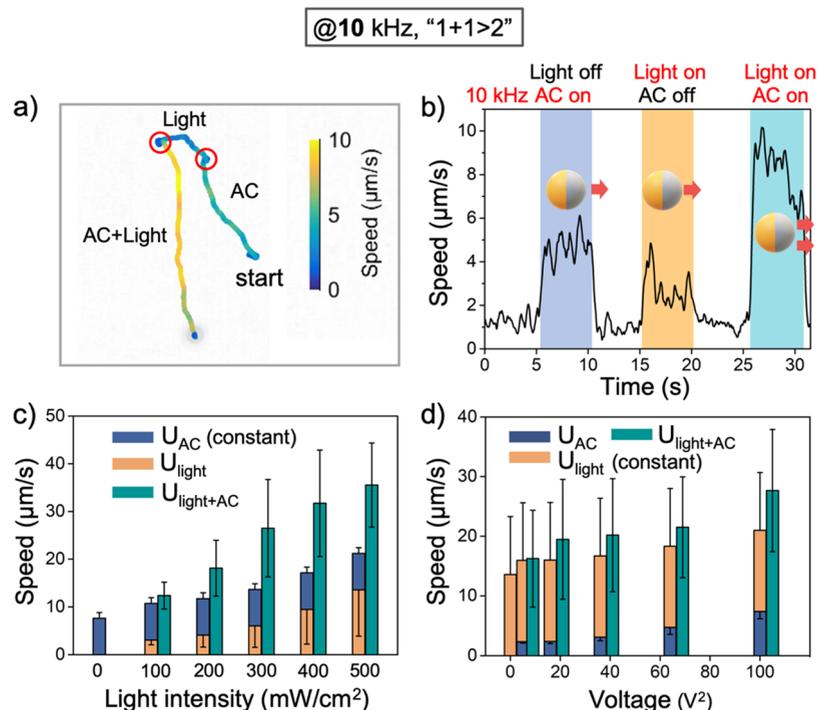
Figure 2. Synergistic propulsion of a TiO₂−Pt micromotor powered by light and 10 kHz AC field. (a, b) Representative trajectory (a) and instantaneous speeds (b) of a TiO₂−Pt micromotor as power sources were varied (see labels for details). Red circles in (a) indicate changes in propulsion modes. (c, d) Speed of a hybrid TiO₂−Pt micromotor (green data) powered by both light (orange) and 10 kHz AC electric field (blue) is significantly higher than the cumulative speed when powered individually. This 1 + 1 > 2 effect applies to experiments conducted at varied light intensities ((c) voltage 10 V) or varied driving voltages ((d) light intensity 500 mW/cm²).

synthesizing TiO₂ microspheres of ∼3 μm in diameter via a template-coating method (with a 3 μm SiO₂ microsphere as the core), then by sputtering Pt on half of the spheres (see Supporting Information for details of synthesis). An important feature is that because Pt and TiO₂ caps absorb and reflect light differently, the TiO₂ cap appears bright while Pt appears dark under an inverted microscope operating in bright field (Figure 1b). One can therefore easily distinguish the Janus interface separating the two hemispheres, a critical feature for our later analysis of the tilting angle (see the Supporting Information and Figure S1 for details). The experiment chamber that enabled two power mechanisms (Figure 1a, center) was constructed by stacking two pieces of conductive indium−tin oxide (ITO) glass slide with a spacer in between. AC electric fields of the maximum field strength of ∼10 V/200 μm, or 5×10^4 V/m, was applied, with frequencies typically ranging from 1 to 100 kHz. UV light of 365 nm, when needed, was applied from above the transparent chamber, and samples were observed and recorded from below with an inverted microscope. An aqueous suspension of TiO₂−Pt microspheres is added to the chamber, without any additional chemicals.

When powered by either source of energy, TiO₂−Pt Janus micromotors moved as expected from our design described above. On the one hand, their speeds scaled more or less linearly with an increase in light intensity when photocatalysis was the sole propulsive force (Figure 1c), agreeing with literature reports,[18,30] because an increase in light intensity leads more photogenerated electrons and holes, a higher photocatalytic reaction rate, stronger fluxes of protons, and therefore a faster motor speed. On the other hand, the speeds scaled roughly to the second power of the applied electric field strength when ICEP (@10 kHz) was solely responsible for its

motion (Figure 1d), consistent with theoretical prediction and earlier studies.[23] In both cases, the motors moved with the TiO₂ forward and in randomized, independent trajectories (Figure S2 and Video S1), indicating autonomous motion and minimal drifting caused by light or electric fields. Moreover, similar to earlier reports, the speeds and directionality of a TiO₂−Pt micromotor can be modulated by varying the driving AC frequencies (Figure 1f): they move with TiO₂ forward via ICEP at ∼10 kHz, come to a stop at ∼100 kHz, and begin to move in the opposite direction toward Pt beyond ∼200 kHz.[31−34] The last regime of reverse motion is not explored in the current manuscript, even though switching a hybrid micromotor between a forward and reverse motion is useful.[14]

A surprising speed enhancement was observed when the two sources of power, UV light and an AC electric field, were applied simultaneously (Figure 2, Video S2). More specifically, we discovered that the speed of a TiO₂−Pt micromotor subject to both light and an AC electric field ($U_{light+AC}$) was always higher than the simple sum of its speed under either propulsion (U_{light} or U_{AC}). For example, such a micromotor moved at 25 μm/s ($U_{light+AC}$) when simultaneously powered by a driving electric potential of 10 V and light intensity of 300 mW/cm², while each propulsion conducted separately propelled a motor at 6 μm/s (U_{light}) and 7 μm/s (U_{AC}), respectively (Figure 2a,b). The simple math of ($U_{light+AC}$ − (U_{light} + U_{AC}))/(U_{light} + U_{AC}) shows that photocatalysis and ICEP synergistically boost the speed of a micromotor by 92%. Such a synergistic enhancement was found across a wide range of experimental parameters, shown in Figure 2c,d by the difference between the green bar and the sum of the yellow and blue bars.
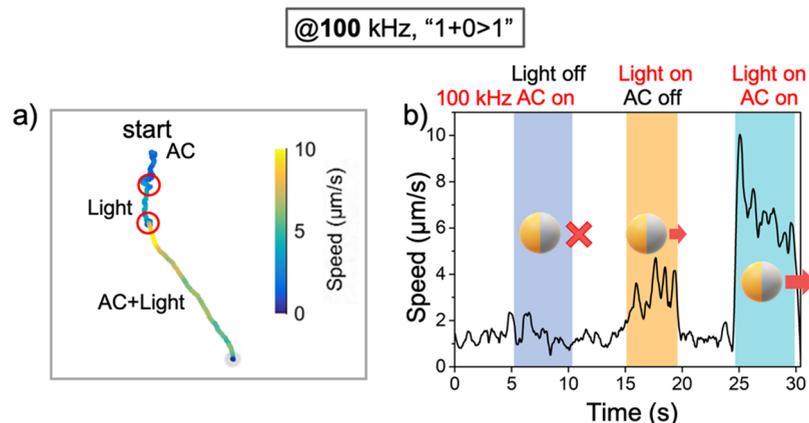
Figure 3. Synergistic propulsion of a TiO$_2$−Pt micromotor powered by light and an 100 kHz AC field. (a, b) Representative trajectory (a) and instantaneous speeds (b) of a TiO$_2$−Pt micromotor as power sources were varied (see labels for details). ICEP becomes negligible at 100 kHz, thus "0". Red circles in (a) indicate changes in propulsion modes.
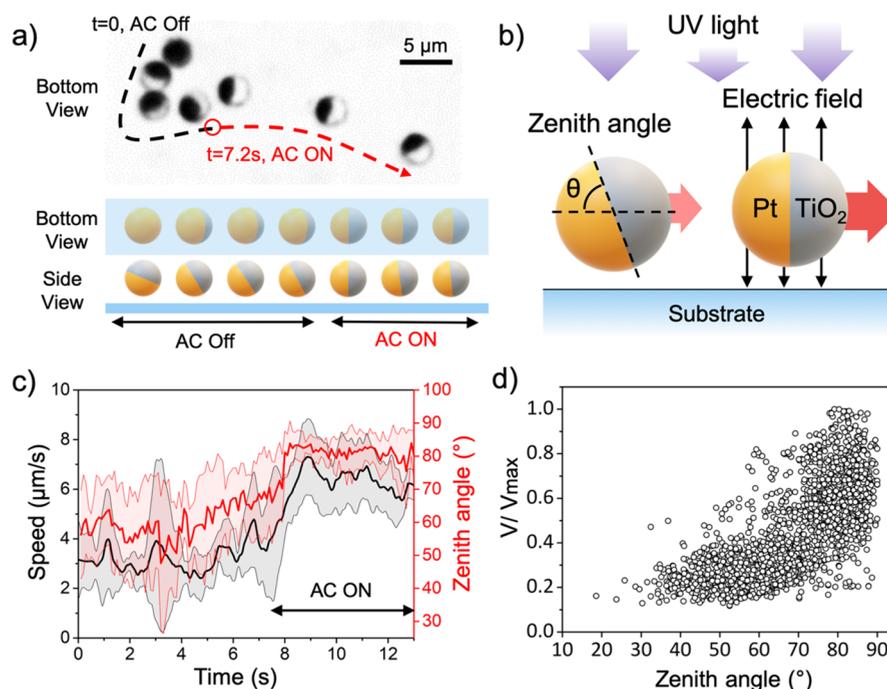

Figure 4. Tilting-induced retardation. (a) Orientation of a TiO$_2$−Pt Janus microsphere moving on a substrate under constant light illumination. This optical micrograph is generated by overlaying seven screenshots of a particle moving for a total of 12 s, imaged with an inverted microscope. A 10 kHz AC electric field was applied from $t = 7.2$ s forward. Cartoon illustrations of its orientations during this period, viewed from the bottom or the side, are given below the actual micrographs. (b) Definition of the zenith angle θ of a Janus microsphere moving near a substrate. When an electric field is applied, this Janus particle reorients its Janus interface to be perpendicular to the substrate. (c) An abrupt change in both θ and the speeds of a TiO$_2$−Pt micromotor is observed as an AC electric field is applied at 7.2 s. Shaded error bars represent standard deviations from five independent micromotors. (d) Monotonic change in motor speeds (normalized to the maximum value of 9.8 μm/s) as the zenith angle changes.

This previously unreported synergy between two seemingly independent propulsion mechanisms for a hybrid micromotor is somewhat counterintuitive. To elaborate, photocatalysis operates by photogenerated electron−hole pairs that react with chemicals on the particle surface, while ICEP is a result of asymmetric polarization and has nothing to do with chemical reactions. One would naively expect these two mechanisms to be orthogonal. However, because they both involve surface electrokinetics (variation in double layers, transport of charged species, and ultimately a slip velocity that drives the particle), the photocatalysis and ICEP mechanisms could in theory be

coupled. To simplify the mechanistic understanding, we first decouple the two mechanisms by examining the speed of a TiO$_2$−Pt micromotor under the light and subject to an AC electric field of 100 kHz, rather than 10 kHz (Figure 3, Video S3). The reasoning is that ions do not catch up at a driving frequency that is high enough, and ICEO as well as ICEP stops. A simple estimate of the threshold frequency for ICEO to occur ω_c is done via $\omega_c = \frac{\lambda R}{D}$,[23] where λ is the double layer thickness, R is the radius of the particle (1.5 μm), and D is the diffusion coefficient of protons (9.31×10^{-9} m^2/s). With measured conductivity values, ω_c is estimated to be 68 and 163
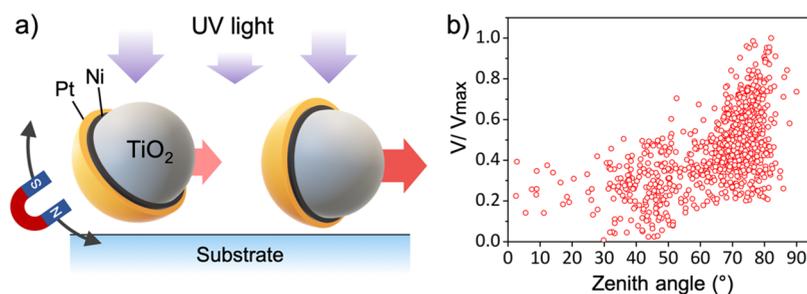
Figure 5. Testing tilting-induced retardation with magnetic fields. (a) Experimental scheme of varying the tilting angle of a TiO_2-Ni/Pt motor with an externally applied magnetic field, enabled by the additional Ni layer below Pt. (b) By continuously varying the zenith angle θ, the speed of a TiO_2-Ni/Pt micromotor under the light (in the absence of any electric fields) changes as a function of θ in a way similar to the case with AC electric fields (Figure 4d). Speeds are normalized to the maximum value of 9.1 μm/s.

kHz for pure water (for data in Figure 1−4) and 5% H_2O_2 (for data in Figure 6), respectively. As a result, we make the reasonable assumption that ICEP becomes negligible at 100 kHz, consistent with the data shown in Figure 1e, and eliminate the possible enhancement of ICEP by light propulsion. The motor moves solely by photocatalysis in this case. However, an increase of 80% in the photoactive motor's speed was registered once the electric field was turned on, that is, $[U_{light+AC} - (U_{light} + 0)]/(U_{light} + 0) = 80\%$. This enhancement in the absence of ICEP, $1 + 0 > 1$, suggests that the observed synergy of $1 + 1 > 2$ is, by its nature, a photoactive micromotor speeding up in an AC electric field, rather than the opposite case of an electrical micromotor speeding up under the light.

There are a few possible ways an electric field could facilitate the photoelectrochemical propulsion of a TiO_2-Pt motor. For example, an electric field could redistribute ions around a TiO_2-Pt microsphere that are critical for its electrophoretic propulsion. However, this interference quickly vanishes at a high AC frequency, such as 100 kHz, where ions cannot catch up, and it can thus be ignored (see the estimate of ω_c above). Alternatively, it is also possible for an electric field to facilitate the electron−hole separation in TiO_2, leading to more efficient photochemistry.[35] However, this mechanism requires a DC electric field along the direction from the Pt to the TiO_2 hemisphere (see Figure 1a) and does not apply in the current system.

After closely examining the orientation of a moving TiO_2- Pt motor before and after an electric field was applied, we propose that a rectification of the tilting angle of a TiO_2-Pt micromotor, in the presence of an electric field, is responsible for the speed enhancement in either the case of $1 + 1 > 2$ or $1 + 0 > 1$. To elaborate, we first note that, as mentioned earlier, a moving TiO_2-Pt Janus motor under an optical microscope displays a clear Janus interface that separates the bright TiO_2 hemisphere from the dark Pt. As it moves under the light without an electric field, one sees a larger portion of the sphere being black (Figure 4a), suggesting that it moves with its Pt hemisphere tilted backward and facing the bottom substrate, that is, a zenith angle θ (defined in Figure 4b) smaller than 90°. Note that, because the TiO_2 side is somewhat transparent, the same optical micrograph could also be interpreted as the Pt hemisphere tilted "forward" and away from the substrate; that is, $\theta > 90°$. However, we postulate that the configuration with $\theta < 90°$, that is, that shown in Figure 4b, is more energetically favorable, because the Pt cap is significantly heavier than water. This preference in a configuration due to a heavier metal cap is

echoed in several experimental studies, where Janus micromotors exhibited negative gravitaxis.[36,37]

When an AC electric field was applied perpendicular to the substrate, however, θ changed to a value close to 90° within 1 s and maintained mostly constant over time, indicating that the Janus micromotor now moves with its Janus interface perpendicular to the substrate and parallel to the applied electric field. Such a transition in θ is presented in Figure 4a, where overlaid optical micrographs illustrate how the Janus interface changed for a TiO_2-Pt micromotor before and after an AC field was applied. Most importantly, Figure 4c shows that the temporal evolution of θ of a TiO_2-Pt Janus particle correlates nicely with the variation in its speed over time, better presented in Figure 4d by relating the motor speed at every instance to its tilting angle θ at that moment. Clearly, the tilt of the Janus interface of a TiO_2-Pt micromotor away from the perpendicular position significantly slows it down, an effect we refer to as tilting-induced retardation. Qualitatively, its speed increases monotonically as its tilting angle is increased and sharply rises to the peak value as the angle approaches 90°.

The above two observations, that a TiO_2-Pt Janus motor moves in a tilted fashion under the light but in the absence of an electric field, and that its θ must change to ~90° once an electric field is applied, can be qualitatively understood as follows. First, two earlier studies have reported that chemically powered bimetallic microrods move near a solid−liquid interface with their long axes tilted away from the substrate.[38,39] In both cases, the nonequilibrium orientation is likely to arise from a complicated interplay among chemical gradients, hydrodynamics, gravity, and electrostatics. Quite a few theoretical/simulation studies also predict a tilted configuration for a phoretically powered Janus microsphere near a solid−liquid interface, yet measurements of these contributions remain challenging. Nevertheless, the fact that certain micromotors powered by chemical gradients move with a particular orientation near a substrate is well-documented, and the photocatalytic TiO_2-Pt micromotor in the current case is no exception.

The alignment of the Janus interface of a metal-dielectric Janus particle parallel to an applied electric field is also a well-known effect (see ref 40 and refs therein). To briefly explain, as the metal cap of a Janus particle is exposed to an applied electric field, the spontaneous electrical polarization prefers a particle orientation that minimizes the total energy of the system. This dictates that the Janus particle aligns its Janus interface parallel to the applied electric field, as revealed by simulations, to generate dipoles of the largest magnitude that maximizes the overall polarization. Notably, the Velev group
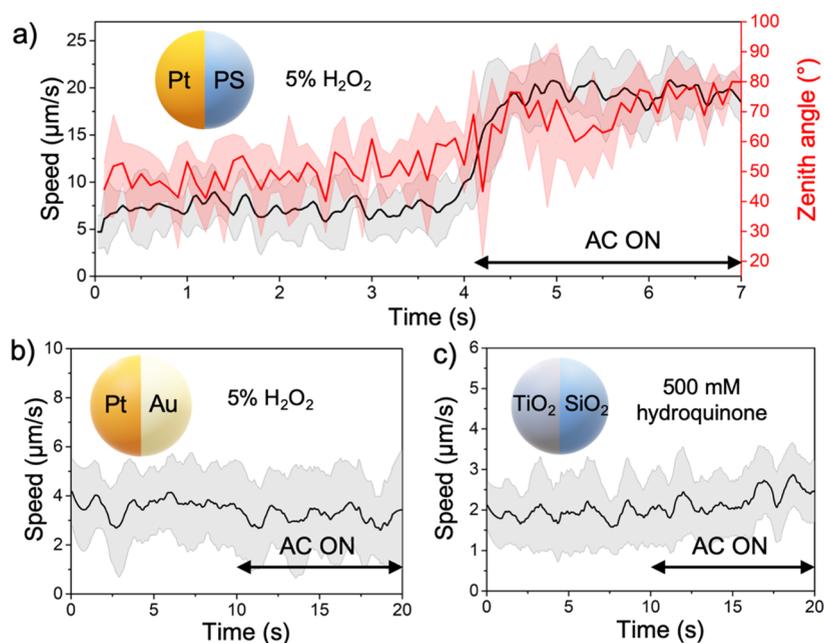
Figure 6. Corroborating tilting-induced retardation with three more types of micromotors: Pt-coated PS microspheres, Pt-coated gold microspheres, and TiO$_2$-coated SiO$_2$ microspheres. Speeds of these three types of micromotors in their respective chemical fuels (hydrogen peroxide in (a, b) and hydroquinone in (c)) before and after the application of 100 kHz of AC electric fields are plotted. Error bars are presented as shades in the data plots.

has exploited this alignment for the assembly of SiO$_2$–Au Janus microspheres into high-order structures such as chains and crystals.[41] This reorientation and alignment, once the electric field is turned on, is also reported in all previous studies of micromotors powered by ICEP.[23,26] A TiO$_2$–Pt microsphere in our case, given its metal-dielectric nature, complies with this feature.

The above argument, that an electric field accelerates an electrophoretic TiO$_2$–Pt micromotor by rectifying its tilt, can be corroborated by an experiment where an approach other than an electric field (e.g., a magnetic field) is used to modulate the tilting angle of a moving TiO$_2$–Pt micromotor and thus its speed (Figure 5, Video S4). This was achieved by first depositing a magnetic Ni layer before the Pt layer during the fabrication of this Janus particle, then exposing this TiO$_2$–Ni/Pt micromotor to an external magnetic field (applied by a hand-held magnet, see the Supporting Information for details). Because the Ni layer magnetizes in the applied magnetic field and becomes polarized, the Janus particle now favors an orientation with a tilting angle θ determined by the externally applied magnetic field. However, unlike the previous case, where the electric field was always applied perpendicular to the substrate (fixing θ to 90°), the magnetic field in the current experiment could be applied in any arbitrary direction, thus enabling a wide range of θ that was inaccessible previously (orientations of $\theta > 90°$ were difficult to realize with this method). As a result, the tilting angle θ of a TiO$_2$–Ni/Pt micromotor under UV light changed with the rotating magnetic field (Figure 5b), leading to a significant change in its speed. This observation agrees nicely with our hypothesis, and the speed and θ are similarly correlated, after normalization, in experiments with either an electric (Figure 4d) or magnetic field (Figure 5b). We confirm that a magnetic field exerts no force but only torque to a micromotor, and it moved only after the light was applied (see Figure S3 for details).

To further support this tilting-induced retardation, the dynamics of three different types of Janus micromotors under an AC electric field were monitored (Figure 6 and Video S5): Pt-coated polystyrene microspheres (Pt-PS, Figure 6a), gold–platinum bimetallic microspheres (Au–Pt, Figure 6b), and TiO$_2$-coated SiO$_2$ microspheres (TiO$_2$–SiO$_2$, Figure 6c). These three types of micromotors of similar shapes and sizes (see the Supporting Information for synthesis and Figure S4 for scanning electron microscopy (SEM) images) were chosen not only because they are popularly studied for fundamental and applied research but also because they carry similarities yet differences to TiO$_2$–Pt micromotors that make them good controls. For example, Pt-PS catalytically decomposes H$_2$O$_2$ into water and oxygen, and the resulting chemical gradient moves the particle likely by combined electrophoresis and diffusiophoresis.[42,43] Similarly, the photogenerated electron–hole pairs from the TiO$_2$ cap of a TiO$_2$–SiO$_2$ motor react with hydroquinone (HQ) and water in the solution, and the resulting concentration gradient powers the motor possibly in the same way as a Pt-PS motor.[44] Finally, a Au–Pt microsphere moves in H$_2$O$_2$ by essentially the same mechanism as a TiO$_2$–Pt motor, where a proton gradient across the microsphere powers it by self-electrophoresis.[45,46] Complications in their respective propulsion mechanisms aside,[11] all three motors thus move by some kind of chemical gradients,[4] just like a TiO$_2$–Pt motor, and could consequently move with a tilt as explained earlier. However, Pt-PS is the only one among the three that has two hemispheres of significantly different polarizability. It is therefore the only one that can be rectified by an electric field and thus behave differently before and after application of an electric field. Au–Pt and TiO$_2$–SiO$_2$, being a metal–metal and dielectric-dielectric Janus microsphere, are unable to generate sufficient torques under an electric field to realign.

Experiments were performed in their respective fuels (labeled in Figure 6, no light was needed) with or without

an AC electric field, and details of these experiments can be found in the Supporting Information. Note that AC electric fields operating at 100 kHz, rather than at 10 kHz, were used in these control experiments to minimize the effect of ICEP that could complicate the particle dynamics (*i.e.*, focusing on the 1 + 0 > 1 scenario). Results in Figure 6 indeed show that Pt-PS micromotors accelerated by over 100% under an AC electric field, while the speeds of Au−Pt or TiO$_2$−SiO$_2$ motors hardly changed under the same condition, consistent with our reasoning above. More specifically, the dynamics of a Pt-PS micromotor before and after the application of an AC field closely resembles that of a TiO$_2$−Pt micromotor, showing a sharp transition of its tilting angle θ and a strong correlation between motor speed and θ. These results support our claim that the speed of a chemically powered micromotor is slowed by its tilt and can be significantly accelerated if this tilt can be rectified (via an electric or magnetic field). Note that two earlier studies reported that Pt-PS micromotors moved on a substrate with a tilting angle of ∼90° (*i.e.*, a vertical Janus interface).[47,48] We tentatively attribute this discrepancy between earlier results and ours to the fact that the tilt of a micromotor is sensitive to experimental conditions and the details of the interaction between chemicals and particle surfaces, emphasized in theoretical studies.

Before we conclude, we acknowledge the reason why tilt slows down a phoretic micromotor, that is, tilting-induced retardation, remains poorly understood at this moment. One naïve possibility is that, because the propulsive force on a tilted micromotor points perpendicular to its equator, by decomposing the force vector into two components along and vertical to the substrate, only part of the total propulsive force contributes to moving the particle along the substrate (Figure S5). This argument logically predicts that the vertical force would lift the micromotor off the substrate (negative gravitaxis), especially at a small θ. Indeed, we often see a TiO$_2$−Pt micromotor move out of focus as light is turned on (Video S6) but not if an electric field is applied that locks its orientation, an observation in seeming agreement with the analysis above. However, this simple geometric argument ignores most of the effects that, as suggested by simulations and theories, contribute to the appearance of a tilted interface, such as hydrodynamics and chemical gradients. This argument also predicts that the motor's speed along on the *xy* plane is proportional to sin θ, which fits poorly with the experimental data in Figure 4d and 5b. A more complete mechanism on the tilting-induced retardation is currently being sought.

CONCLUSIONS

In conclusion, we have discovered a surprising enhancement in the speed of a micromotor by up to 90% when it is powered by both UV light and an AC electric field. We proposed a mechanism based on the tilting of an electrokinetically driven micromotor near a substrate, where applying an electric field (at low or high driving frequencies) rectifies the tilt and enhances the motor speed. Control experiments with magnetic fields and three types of micromotors strongly support this mechanism. This unexpected tilting-induced retardation is suspected to be a general feature for many chemically powered micromachines, suggesting a viable strategy to significantly improve their performance by reorienting the Janus particle with electromagnetic fields. Future efforts include experiments in unconfined spaces and a better elucidation of why tilting affects motor speeds. Our finding could also shed light on the

fundamental understanding of the interactions between active matter and their complex environments that not only give rise to tilting but is also relevant for many interesting collective behaviors.

METHODS/EXPERIMENTAL

Preparation of TiO$_2$ Microspheres. TiO$_2$ microspheres were prepared by coating SiO$_2$ microspheres with a thin (50−100 nm) layer of TiO$_2$, with tetrabutyl titanate as a precursor, following a previously reported protocol.[49,50] Two solutions were prepared. First, 90 μL of tetrabutyl titanate (Aladin No. T104105) was dissolved in 2.5 mL of ethanol (Aladin No. E111994); then, 300 μL of SiO$_2$ microspheres (3 μm, 5 vt%, Baseline No. 6-7-0200) and 20 μL of isomeric alcohol ethoxylates (0.1 M, BASF) were dispersed in 2.5 mL of ethanol. The diluted TiO$_2$ precursor solution and SiO$_2$ microsphere dispersion were then mixed by vigorous shaking using a vortex mixer. The mixture was then sonicated for 30 min and let to react at room temperature for 2 h. Then, TiO$_2$ microspheres were collected by centrifugation at 4000 rpm for 5 min and washed repeatedly with ethanol and pure water (18.2 MΩ·cm) each for three times. Anatase TiO$_2$ microspheres were obtained after they were annealed for 2 h at 450 °C. A more detailed synthesis and characterization will be reported in a separate study.

Preparation of Au Microspheres. Au microspheres were chemically synthesized following an earlier report.[51] First, 1 mL of chloroauric acid solution (0.6 g/mL) was dissolved in 2 mL of Arabic gum solution (5.25 mg/mL) to obtain solution A. Then, 0.475 g of ascorbic acid was dissolved in 9 mL of Arabic gum solution (7 mg/mL) to obtain solution B. Solutions A and B were then vigorously mixed by a vortex mixer. The mixed solution turned brown immediately. Then, Au microspheres were collected by centrifugation at 4000 rpm for 5 min and washed repeatedly with ethanol and pure water (18.2 MΩ·cm) each for three times. A representative SEM image of the synthesized Au microsphere can be found in Figure S4c.

Preparation of TiO$_2$−Pt, PS-Pt, and Au−Pt Janus microspheres. TiO$_2$−Pt, PS-Pt, and Au−Pt Janus micromotors were prepared by sputtering Pt on one-half of the synthesized microspheres. PS microspheres were purchased from Huge (2 μm, 10 vt %, No. DRM02). Microspheres were first suspended in ethanol (20 μL) and dispersed by ultrasound. The suspension was then drop-casted on a piece of clean glass slide to obtain a monolayer. Janus microspheres were prepared by sputtering a thin (∼50 nm) Pt layer on top of the monolayer (HHV TF500), followed by sonication and resuspension in deionized water.

Preparation of SiO$_2$−TiO$_2$ Janus Microspheres. SiO$_2$−TiO$_2$ micromotors were prepared by depositing a layer of TiO$_2$ on one-half of SiO$_2$ microspheres. SiO$_2$ microspheres (3 μm, 5 vt %, Baseline No. 6-7-0200) were first suspended in ethanol (20 μL) and dispersed by sonication. The suspension was then drop-casted on a piece of clean glass slide to obtain a monolayer of SiO$_2$. SiO$_2$−TiO$_2$ motors were prepared by sputtering a thin TiO$_2$ layer on top of the SiO$_2$ monolayer (HHV TF500). These Janus microspheres were annealed for 2 h at 450 °C to convert TiO$_2$ to the anatase phase.

Motor Experiment and Experimental Setup. Micromotors were dispersed in deionized water before use. PS-Pt and Au−Pt micromotors suspensions were mixed with 30% H$_2$O$_2$ to obtain 5% H$_2$O$_2$ solution. SiO$_2$−TiO$_2$ micromotors were mixed with hydroquinone to obtain 500 mM hydroquinone solution.

For the electric field experiment, a cylindrical experimental cell (200 μm tall and 5 mm in diameter) was constructed by stacking a silicone spacer with a circular through-hole between two ITO glass slides (see Figure 1a for a schematic). Then 5.5 μL of micromotor suspension was transferred by a pipet to the experimental cell. The two ITO slides were wired to a wave generator (Keysight 33500B). The frequency was tuned from 10 to 1000 kHz, and the voltage was tuned between 0 and 10 V$_{p-p}$.

For the experiment with light, UV light of 365 nm was generated by a light-emitting diode (LED) lamp (Thorlabs, M365LP1-C1) with a power density ranging from 100 to 500 mW/cm^2.

For the magnetic field experiment, a hand-held magnet was placed around the experimental chamber to magnetize the sample from different directions.

Data Collection and Analysis. The motion of motors was observed under an inverted optical microscope (Olympus IX73) and recorded by a Point Gray camera (FL3-U3-13E4C-C) at a frame rate of 30 frames per second. The videos were processed and analyzed by MATLAB to yield the *x-y* coordinates of each motor and their instantaneous speeds (codes courtesy of Prof. Hepeng Zhang from Shanghai Jiaotong University).

To obtain the tilting angle of the Janus motor, the zenith angle θ was calculated from the pixel intensity of the optical micrographs (see Figure S1 for schematic). To elaborate, motors moving with different zenith angles show distinct moon phases in the optical micrographs. According to literature,[52] the zenith angle θ can be calculated approximately by the following equation

$$B = \frac{A}{2}(1 + \cos \theta) \qquad (1)$$

where A is the brightness of the motor when the zenith angle is 0 (*i.e.*, the motor is completely dark in the optical micrograph, Figure S1,i), and B is the brightness of the motor with a nonzero zenith angle (Figure S1,ii). The brightness of a motor is acquired from imageJ (https://imagej.nih.gov/ij/) by averaging the pixel intensity value within the recognized boundary of a micromotor. In practice, the value A is hard to directly acquire from an optical image, because a moving Janus motor is rarely completely dark. We therefore assumed that $\theta = 90°$ (corresponding to a half-moon phase) when an electric field is applied and doubled the brightness value in this case to obtain A.

ASSOCIATED CONTENT

ⓈⒾ Supporting Information

The Supporting Information is available free of charge at https://pubs.acs.org/doi/10.1021/acsnano.0c03022.

> TiO_2−Pt moving under an AC electric field or light separately (MP4)
>
> TiO_2−Pt moving under a 10 kHz AC electric field and light simultaneously (MP4)
>
> TiO_2−Pt moving under a 100 kHz AC electric field and light simultaneously. There is a very small propulsive force when light is turned off and 100 kHz AC field is on (MP4)
>
> TiO_2−Ni/Pt moving under a magnetic field and light simultaneously. This video highlights the fact that the tilt of a motor, which is modified by the external magnetic field, can significantly slow a motor (MP4)
>
> Pt−PS, Au−Pt, or TiO_2−SiO_2 micromotors moving under an AC electric field. Metal-dielectric Janus particles are mixed as references to indicate the moment of turning on the AC electric field, as well as to show the absence of any electric propulsion (MP4)
>
> TiO_2−Pt micromotors moving out of focus as light is turned on (MP4)
>
> Schematic of the moon phases and corresponding zenith angles, trajectories of TiO_2−Pt motors under AC electric fields or light, trajectories of TiO_2−Ni/Pt motors under magnetic fields, SEM of three types of micromotors used as controls, schematic of the propulsive force acting on a TiO_2−Pt micromotor (PDF)

AUTHOR INFORMATION

Corresponding Author

Wei Wang − *School of Materials Science and Engineering, Harbin Institute of Technology (Shenzhen), Shenzhen 518055, China;* ⓞ orcid.org/0000-0003-4163-3173; Email: weiwangsz@hit.edu.cn

Authors

Zuyao Xiao − *School of Materials Science and Engineering, Harbin Institute of Technology (Shenzhen), Shenzhen 518055, China*

Shifang Duan − *School of Materials Science and Engineering, Harbin Institute of Technology (Shenzhen), Shenzhen 518055, China*

Pengzhao Xu − *School of Materials Science and Engineering, Harbin Institute of Technology (Shenzhen), Shenzhen 518055, China*

Jingqin Cui − *Pen-Tung Sah Institute of Micro-Nano Science and Technology, Xiamen University, Xiamen 361005, China;* ⓞ orcid.org/0000-0003-4382-6411

Hepeng Zhang − *School of Physics and Astronomy and Institute of Natural Sciences, Shanghai Jiao Tong University, Shanghai 200240, China; Collaborative Innovation Center of Advanced Microstructures, Nanjing 210093, China*

Complete contact information is available at: https://pubs.acs.org/10.1021/acsnano.0c03022

Notes

The authors declare no competing financial interest.

REFERENCES

(1) Chen, X.; Zhou, C.; Wang, W. Colloidal Motors 101: A Beginner's Guide to Colloidal Motor Research. *Chem. - Asian J.* **2019**, *14*, 2388−2405.

(2) Wang, J. *Nanomachines: Fundamentals and Applications;* John Wiley & Sons: Hoboken, NJ, 2013.

(3) Mallouk, T. E.; Sen, A. Powering Nanorobots. *Sci. Am.* **2009**, *300*, 72−77.

(4) Wang, W.; Duan, W.; Ahmed, S.; Mallouk, T. E.; Sen, A. Small Power: Autonomous Nano-and Micromotors Propelled by Self-Generated Gradients. *Nano Today* **2013**, *8*, 531−554.

(5) Medina-Sánchez, M.; Magdanz, V.; Guix, M.; Fomin, V. M.; Schmidt, O. G. Swimming Microrobots: Soft, Reconfigurable, and Smart. *Adv. Funct. Mater.* **2018**, *28*, 1707228.

(6) Hu, C.; Pané, S.; Nelson, B. J. Soft Micro-and Nanorobotics. *Annu. Rev. Control Robot. Auton. Syst.* **2018**, *1*, 53−75.

(7) Katuri, J.; Ma, X.; Stanton, M. M.; Sánchez, S. Designing Micro-and Nanoswimmers for Specific Applications. *Acc. Chem. Res.* **2017**, *50*, 2−11.

(8) Aranson, I. S. Active Colloids. *Phys.-Usp.* **2013**, *56*, 79.

(9) Li, J.; Esteban-Fernandez de Avila, B.; Gao, W.; Zhang, L.; Wang, J. Micro/Nanorobots for Biomedicine: Delivery, Surgery, Sensing, and Detoxification. *Sci. Robot.* **2017**, *2*, eaam6431.

(10) Parmar, J.; Vilela, D.; Villa, K.; Wang, J.; Sanchez, S. Micro-and Nanomotors as Active Environmental Microcleaners and Sensors. *J. Am. Chem. Soc.* **2018**, *140*, 9317−9331.

(11) Wang, W.; Lv, X.; Moran, J. L.; Duan, S.; Zhou, C. A Practical Guide to Active Colloids: Choosing Synthetic Model Systems for Soft Matter Physics Research. *Soft Matter* **2020**, *16*, 3846−3868.

(12) Bechinger, C.; Di Leonardo, R.; Löwen, H.; Reichhardt, C.; Volpe, G.; Volpe, G. Active Particles in Complex and Crowded Environments. *Rev. Mod. Phys.* **2016**, *88*, No. 045006.

(13) Xiao, Z.; Wei, M.; Wang, W. A Review of Micromotors in Confinements: Pores, Channels, Grooves, Steps, Interfaces, Chains, and Swimming in the Bulk. *ACS Appl. Mater. Interfaces* **2019**, *11*, 6667−6684.

(14) Chen, C.; Soto, F.; Karshalev, E.; Li, J.; Wang, J. Hybrid Nanovehicles: One Machine, Two Engines. *Adv. Funct. Mater.* **2019**, *29*, 1806290.

(15) Chen, C.; Tang, S.; Teymourian, H.; Karshalev, E.; Zhang, F.; Li, J.; Mou, F.; Liang, Y.; Guan, J.; Wang, J. Chemical/Light-Powered Hybrid Micromotors with "On-the-Fly" Optical Brakes. *Angew. Chem.* **2018**, *130*, 8242−8246.

(16) Wang, W.; Duan, W.; Zhang, Z.; Sun, M.; Sen, A.; Mallouk, T. E. A Tale of Two Forces: Simultaneous Chemical and Acoustic Propulsion of Bimetallic Micromotors. *Chem. Commun.* **2015**, *51*, 1020−1023.

(17) Popescu, M. N.; Uspal, W. E.; Domínguez, A.; Dietrich, S. Effective Interactions between Chemically Active Colloids and Interfaces. *Acc. Chem. Res.* **2018**, *51*, 2991−2997.

(18) Dong, R.; Zhang, Q.; Gao, W.; Pei, A.; Ren, B. Highly Efficient Light-Driven TiO_2−Au Janus Micromotors. *ACS Nano* **2016**, *10*, 839−844.

(19) Mou, F.; Kong, L.; Chen, C.; Chen, Z.; Xu, L.; Guan, J. Light-Controlled Propulsion, Aggregation and Separation of Water-Fuelled TiO2/Pt Janus Submicromotors and Their "On-the-Fly" Photocatalytic Activities. *Nanoscale* **2016**, *8*, 4976−4983.

(20) Maric, T.; Nasir, M. Z. M.; Webster, R. D.; Pumera, M. Tailoring Metal/TiO_2 Interface to Influence Motion of Light-Activated Janus Micromotors. *Adv. Funct. Mater.* **2020**, *30*, 1908614.

(21) Leeth Holterhoff, A.; Girgis, V.; Gibbs, J. G. Material-Dependent Performance of Fuel-Free, Light-Activated, Self-Propelling Colloids. *Chem. Commun.* **2020**, *56*, 4082−4085.

(22) Xiao, Z.; Chen, J.; Duan, S.; Lv, X.; Wang, J.; Ma, X.; Tang, J.; Wang, W. Bimetallic Coatings Synergistically Enhance the Speeds of Photocatalytic TiO_2 Micromotors. *Chem. Commun.* **2020**, *56*, 4728−4731.

(23) Gangwal, S.; Cayre, O. J.; Bazant, M. Z.; Velev, O. D. Induced-Charge Electrophoresis of Metallodielectric Particles. *Phys. Rev. Lett.* **2008**, *100*, No. 058302.

(24) Nishiguchi, D.; Sano, M. Mesoscopic Turbulence and Local Order in Janus Particles Self-Propelling under an AC Electric Field. *Phys. Rev. E* **2015**, *92*, No. 052309.

(25) Zhang, L.; Xiao, Z.; Chen, X.; Chen, J.; Wang, W. Confined 1D Propulsion of Metallodielectric Janus Micromotors on Micro-electrodes under Alternating Current Electric Fields. *ACS Nano* **2019**, *13*, 8842−8853.

(26) Yan, J.; Han, M.; Zhang, J.; Xu, C.; Luijten, E.; Granick, S. Reconfiguring Active Particles by Electrostatic Imbalance. *Nat. Mater.* **2016**, *15*, 1095.

(27) Boymelgreen, A. M.; Balli, T.; Miloh, T.; Yossifon, G. Active Colloids as Mobile Microelectrodes for Unified Label-Free Selective Cargo Transport. *Nat. Commun.* **2018**, *9*, 760.

(28) Lee, J. G.; Brooks, A. M.; Shelton, W. A.; Bishop, K. J.; Bharti, B. Directed Propulsion of Spherical Particles along Three Dimensional Helical Trajectories. *Nat. Commun.* **2019**, *10*, 1−8.

(29) Wang, S.; Ma, F.; Zhao, H.; Wu, N. Bulk Synthesis of Metal−Organic Hybrid Dimers and Their Propulsion under Electric Fields. *ACS Appl. Mater. Interfaces* **2014**, *6*, 4560−4569.

(30) Jang, B.; Hong, A.; Kang, H. E.; Alcantara, C.; Charreyron, S.; Mushtaq, F.; Pellicer, E.; Büchel, R.; Sort, J.; Lee, S. S.; et al. Multiwavelength Light-Responsive Au/B-TiO_2 Janus Micromotors. *ACS Nano* **2017**, *11*, 6146−6154.

(31) Boymelgreen, A.; Yossifon, G.; Miloh, T. Propulsion of Active Colloids by Self-Induced Field Gradients. *Langmuir* **2016**, *32*, 9540−9547.

(32) Shields, C. W., IV; Han, K.; Ma, F.; Miloh, T.; Yossifon, G.; Velev, O. D. Supercolloidal Spinners: Complex Active Particles for Electrically Powered and Switchable Rotation. *Adv. Funct. Mater.* **2018**, *28*, 1803465.

(33) Shen, C.; Jiang, Z.; Li, L.; Gilchrist, J. F.; Ou-Yang, H. D. Frequency Response of Induced-Charge Electrophoretic Metallic Janus Particles. *Micromachines* **2020**, *11*, 334.

(34) Hashemi Amrei, S. M. H.; Miller, G. H.; Ristenpart, W. D. Asymmetric Rectified Electric Fields Generate Flows that Can Dominate Induced-Charge Electrokinetics. *Phys. Rev. Fluids* **2020**, *5*, No. 013702.

(35) Jiang, Z.; Wang, H.; Huang, H.; Cao, C. Photocatalysis Enhancement by Electric Field: TiO_2 Thin Film for Degradation of Dye X-3B. *Chemosphere* **2004**, *56*, 503−508.

(36) Takatori, S. C.; De Dier, R.; Vermant, J.; Brady, J. F. Acoustic Trapping of Active Matter. *Nat. Commun.* **2016**, *7*, 10694.

(37) Campbell, A. I.; Ebbens, S. J. Gravitaxis in Spherical Janus Swimming Devices. *Langmuir* **2013**, *29*, 14066−14073.

(38) Brosseau, Q.; Usabiaga, F. B.; Lushi, E.; Wu, Y.; Ristroph, L.; Zhang, J.; Ward, M.; Shelley, M. J. Relating Rheotaxis and Hydrodynamic Actuation Using Asymmetric Gold-Platinum Phoretic Rods. *Phys. Rev. Lett.* **2019**, *123*, 178004.

(39) Ren, L.; Zhou, D.; Mao, Z.; Xu, P.; Huang, T. J.; Mallouk, T. E. Rheotaxis of Bimetallic Micromotors Driven by Chemical−Acoustic Hybrid Power. *ACS Nano* **2017**, *11*, 10591−10598.

(40) Velev, O. D.; Gangwal, S.; Petsev, D. N. Particle-Localized AC and DC Manipulation and Electrokinetics. *Annu. Rep. Prog. Chem., Sect. C: Phys. Chem.* **2009**, *105*, 213−246.

(41) Gangwal, S.; Cayre, O. J.; Velev, O. D. Dielectrophoretic Assembly of Metallodielectric Janus Particles in AC Electric Fields. *Langmuir* **2008**, *24*, 13312−13320.

(42) Ebbens, S. J.; Howse, J. R. Direct Observation of the Direction of Motion for Spherical Catalytic Swimmers. *Langmuir* **2011**, *27*, 12293−12296.

(43) Howse, J. R.; Jones, R. A.; Ryan, A. J.; Gough, T.; Vafabakhsh, R.; Golestanian, R. Self-Motile Colloidal Particles: From Directed Propulsion to Random Walk. *Phys. Rev. Lett.* **2007**, *99*, No. 048102.

(44) Singh, D. P.; Choudhury, U.; Fischer, P.; Mark, A. G. Non-Equilibrium Assembly of Light-Activated Colloidal Mixtures. *Adv. Mater.* **2017**, *29*, 1701328.

(45) Wheat, P. M.; Marine, N. A.; Moran, J. L.; Posner, J. D. Rapid Fabrication of Bimetallic Spherical Motors. *Langmuir* **2010**, *26*, 13052−13055.

(46) Theurkauff, I.; Cottin-Bizonne, C.; Palacci, J.; Ybert, C.; Bocquet, L. Dynamic Clustering in Active Colloidal Suspensions with Chemical Signaling. *Phys. Rev. Lett.* **2012**, *108*, 268303.

(47) Das, S.; Garg, A.; Campbell, A. I.; Howse, J.; Sen, A.; Velegol, D.; Golestanian, R.; Ebbens, S. J. Boundaries Can Steer Active Janus Spheres. *Nat. Commun.* **2015**, *6*, 8999.

(48) Simmchen, J.; Katuri, J.; Uspal, W. E.; Popescu, M. N.; Tasinkevych, M.; Sánchez, S. Topographical Pathways Guide Chemical Microswimmers. *Nat. Commun.* **2016**, *7*, 10598.

(49) Demirörs, A. F.; van Blaaderen, A.; Imhof, A. A General Method to Coat Colloidal Particles with Titania. *Langmuir* **2010**, *26*, 9297−9303.

(50) Xu, P.; Duan, S.; Xiao, Z.; Yang, Z.; Wang, W., Light-powered Active Colloids from Monodisperse and Highly Tunable Micro-spheres with A Thin TiO_2 shell, *Soft Matter*, ASAP.2020 DOI: 10.1039/D0SM00719F

(51) Goia, D.; Matijević, E. Tailoring the Particle Size of Monodispersed Colloidal Gold. *Colloids Surf., A* **1999**, *146*, 139−152.

(52) Anthony, S. M.; Hong, L.; Kim, M.; Granick, S. Single-Particle Colloid Tracking in Four Dimensions. *Langmuir* **2006**, *22*, 9812−9815.